^{15}N and ^{133}Cs Solid NMR Studies on Ionic Dynamics in Plastic $CsNO_2$*

H. Honda[a], M. Kenmotsu[a], N. Onoda-Yamamuro[a], H. Ohki[a], S. Ishimaru[a], R. Ikeda, and Y. Furukawa[b]

[a] Department of Chemistry, University of Tsukuba, Tsukuba 305, Japan
[b] Faculty of School Education, Hiroshima University, Higashi-Hiroshima 739, Japan

Z. Naturforsch. **51a**, 761–768 (1996); received October 24, 1995

The temperature dependence of the ^{15}N and ^{133}Cs NMR spin-lattice relaxation times, the ^{15}N spin-spin relaxation time, and the ^{15}N and ^{133}Cs spectra of $CsNO_2$ was observed in the plastic phase ($209.2 < T < 673$ K (m. p.)) and the low-temperature phase (Phase II). In Phase II we found the NO_2^- 180°-flip, which could be attributed to the anomalous increase of the heat capacity curve, and determined the activation energy of this motion to be 8.7-11.7 kJ mol^{-1}. The ^{15}N and ^{133}Cs spectra in this phase are inconsistent with the reported crystal structure $R\bar{3}m$ and can be explained by lower crystal symmetry. In the plastic phase we detected a new anionic motion with 11 kJ mol^{-1}, an isotropic NO_2^- reorientation with 8.5-9 kJ mol^{-1}, and ionic self-diffusion with 47 kJ mol^{-1}. The presence of ionic self-diffusion was confirmed by measuring the electrical conductivity.

Key words: ^{15}N and ^{133}Cs Solid NMR, Plastic crystal, Phase transition, Chemical shift anisotropy, Electric field gradient.

1. Introduction

The nitrites MNO_2 (M = K, Rb, Cs, Tl) are ionic crystals showing plastic phases [1 - 8]. The dynamic properties of potassium [9], rubidium [10], and thallium [11] nitrite in the plastic phase, such as molecular diffusion and isotropic reorientation, are quite analogous to those in molecular plastic phases [12]. The onset of isotropic reorientation of the NO_2^- ions in the plastic phase enables the highly symmetric NaCl or CsCl type cubic structure. At the transition from the low-temperature phase of these nitrites, the heat capacity exhibits an anomalous long tail on the low-temperature side extending over 100 K [2 - 4, 6 - 8]. This anomaly implies that the disorder in structure takes place far below the transition point.

Two solid phases in $CsNO_2$ have been reported [1 - 5]. The plastic phase (Phase I) obtainable between 209.2 and 673 K (melting point) forms a CsCl-type cubic lattice with space group $Pm\bar{3}m$ and $a_0 = 438.9$ pm [1]. Raman [3, 4] and neutron powder diffraction [13] studies have revealed the presence of the two kinds of NO_2^- reorientation motions in Phase I. The transition entropy from Phase II to I amounts to 17.3 J K^{-1} mol^{-1} and is almost the same as the melting entropy (17.79 J K^{-1} mol^{-1}) [2 - 5]. Phase II has a rhombohedral lattice with $R\bar{3}m$ and $a_0 = 430.7$ pm, $\alpha = 87.22°$ [1]. The dielectric constant in this phase [3, 4] shows a marked dispersion attributable to some anionic motion with an activation energy of 13.8 kJ mol^{-1}. The freezing of this motion is expected to occur at the glass transition at ≈ 40 K [3, 4].

In the present study we have studied temperature dependences of the ^{15}N and ^{133}Cs NMR spectra and relaxation times to get information about the NO_2^- motional modes in Phase II and the plastic phase.

2. Experimental

$CsNO_2$ and $Cs^{15}NO_2$ were prepared from $NaNO_2$ (Wako Pure Chemical Industries Ltd.) and $Na^{15}NO_2$ (99 wt% ^{15}N, ICON Inc.), respectively, using a cation exchange resin (Diaion SK-1, Mitsubishi Kasei Corp.). A small amount of $^{15}NO_3^-$ ions involved in the $Cs^{15}NO_2$ eluent was removed by an anion exchange resin (Dowex 1-X8, The Dow Chemical Company).

* Presented at the XIIIth International Symposium on Nuclear Quadrupole Interactions, Providence, Rhode Island, USA, July 23-28, 1995.

Reprint requests to Prof. R. Ikeda, Fax: 81-298-53-6503.

0932-0784 / 96 / 0500-0761 $ 06.00 © – Verlag der Zeitschrift für Naturforschung, D-72072 Tübingen

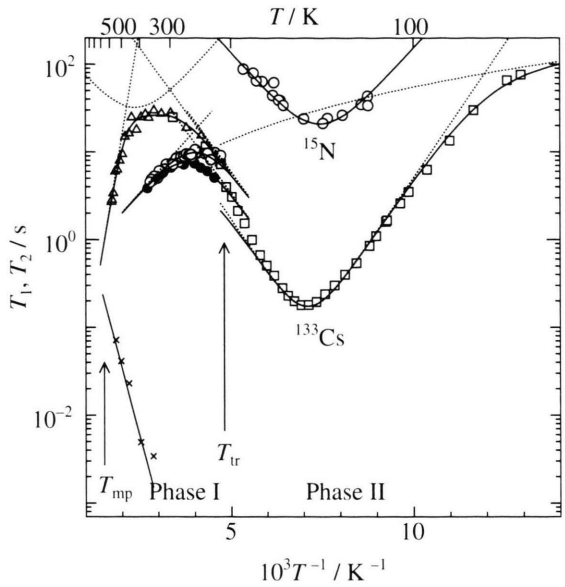

Fig. 1. Temperature dependences of ^{15}N NMR spin-lattice relaxation time T_1 at the Larmor frequencies of 30.42 (○) and 40.56 MHz (●), and spin-spin relaxation time T_2 (×) at 40.56 MHz in $Cs^{15}NO_2$, and ^{133}Cs T_1 at 7.60 (△) and 35.58 MHz (□) in $Cs^{14}NO_2$. Solid and dotted lines are the best fitted theoretical values. T_{tr} and T_{mp} are the phase transition and melting temperatures, respectively.

Recrystallization of the obtained crude crystals from water gave hygroscopic pale yellow crystals.

^{15}N (I = 1/2) NMR spectra and spin-lattice relaxation time T_1 were measured at the Larmor frequencies 30.42 MHz (7.041 T) and 40.56 MHz (9.388 T) using a Bruker MSL-300 spectrometer at 120-360 K, and a Bruker MSL-400 spectrometer at 220-360 K, respectively. The spin-spin relaxation time T_2 was observed at 300-650 K. The saturation recovery and Carr-Purcell methods were employed for evaluating T_1 and T_2, respectively. The ^{15}N chemical shift was determined using an external reference of $^{15}NH_4^+$ (δ_s = –354 ppm) in a 4.5 M solution of $^{15}NH_4NO_3$ in 3 M hydrochloric acid.

The ^{133}Cs (I = 7/2) NMR T_1 in $Cs^{14}NO_2$ was measured at 35.58 MHz by a homemade spectrometer equipped with an Oxford superconducting magnet (6.37 T) in the range 77-296 K, at 7.6 MHz using a Varian V-7300 electromagnet in the range 213-587 K, and at 52.48 MHz by use of a Bruker MSL-400 in the range 217-384 K; the inversion and saturation recovery methods were employed. We could determine a single value of ^{133}Cs T_1 in the whole temperature range because almost an exponential decay of the magnetization after the 90° pulse was observed. The ^{133}Cs NMR spectrum was obtained from a FID after one 90° pulse at 39.36 MHz using a Bruker MSL-300 spectrometer in the range 130-340 K.

X-ray powder diffraction patterns were recorded at 110 and 298 K by a Philips X'Pert PW 3040/00 diffractometer with a Cu anticathode.

The electrical conductivity was measured at 1 kHz by the two-terminal method using a Yokogawa Hewlett-Packard 4261A LCR meter at 300-620 K. The powdered sample was pressed into a disc, 1 cm in diameter and *ca.* 1 mm thick, and graphite electrodes (Acheson Electrodag 199) were employed.

3. Results and discussion

3.1. Phase II (Low-Temperature Phase)

Temperature dependences of ^{15}N T_1 and T_2 in $Cs^{15}NO_2$ together with ^{133}Cs T_1 in $Cs^{14}NO_2$ in Phase I and II are shown in Figure 1. A shallow ^{15}N T_1 minimum of *ca.* 20 s and a deep ^{133}Cs T_1 minimum of *ca.* 200 ms were observed in Phase II.

^{133}Cs NMR Relaxation Time and Spectra in $Cs^{14}NO_2$

The deep ^{133}Cs T_1 minimum at 140 K is explainable by a quadrupolar mechanism caused by the EFG (electric field gradient) fluctuation at the Cs nuclei due to some anionic motion. A mechanism due to the averaging of magnetic dipole interactions of Cs–Cs and/or Cs–N nuclei can not explain the observed short T_1 minimum. The shallow ^{15}N T_1 minimum at nearly the same temperature is attributable to the same motion giving the ^{133}Cs T_1 minimum.

The asymmetric ^{133}Cs T_1 curve observed in phase II can be expressed by

$$\frac{1}{T_1} = \frac{1}{T_{1\mathrm{Mot}}} + \frac{1}{T_{1\mathrm{Lat}}}, \tag{1}$$

where $T_{1\mathrm{Mot}}$ is due to the NO_2^- motion and $T_{1\mathrm{Lat}}$ to lattice vibrations at low temperatures. Assuming a Debye-type density spectrum for the relaxation of quadrupole nuclei with non-integer spins, we have [14]

$$\frac{1}{T_{1\mathrm{Mot}}} = C\frac{\tau}{1+\omega_{\mathrm{Cs}}^2\tau^2}, \tag{2}$$

Phase	Motional Mode	E_a / kJ mol^{-1}	τ_0 / s	Observation
II	180°-Flip	8.7±2	2.2×10^{-12}	^{15}N T_1
		11.7±2	2.2×10^{-13}	^{133}Cs T_1
I	C_2-Reorientation	11±2		^{133}Cs T_1
		11*		^{15}N T_1
	Isotropic Reorientation	9.0±2		^{15}N T_1
		9.0±2	1.6×10^{-9}	^{133}Cs T_1
	Self-Diffusion	47±2		^{133}Cs T_1
		33±3		^{15}N T_2

Table 1. Motional modes, activation energies (E_a) and the pre-exponential factors (τ_0) for NO_2^- ions derived from spin-lattice and spin-spin relaxation times (T_1, T_2) of ^{15}N in $Cs^{15}NO_2$ and ^{133}Cs T_1 in $Cs^{14}NO_2$.

* The same value evaluated from ^{133}Cs T_1 data was assumed.

while the contribution from lattice vibrations is given by [14]

$$\frac{1}{T_{1\mathrm{Lat}}} = AT^2. \tag{3}$$

Here, C, τ, and ω_{Cs} are a constant depending on the motional mode, the correlation time of the motion, and the ^{133}Cs angular Larmor frequency, respectively. We assume an Arrhenius-type temperature dependence of τ:

$$\tau = \tau_0 \exp \frac{E_a}{RT}. \tag{4}$$

We fitted the (1) - (4) to the observed ^{133}Cs T_1 data and showed the obtained best-fitted T_1 curve in Figure 1.

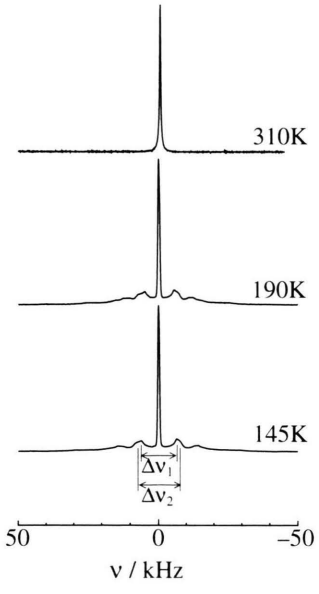

Fig. 2. ^{133}Cs NMR spectra observed at 39.36 MHz in Phase I and Phase II of $Cs^{14}NO_2$. $\Delta\nu_1$ and $\Delta\nu_2$ are linewidths of the first satellite.

Small deviations from the experimental data seen in the high-temperature range of the T_1 minimum can be attributed to the influence of the phase transition. The evaluated activation parameters are listed in Table 1.

The temperature dependence of the recorded ^{133}Cs NMR spectra is shown in Figure 2. The observed lineshapes exhibit typical patterns with non-zero values of the quadrupole coupling constant (e^2Qq) and the asymmetry parameter (η). ^{133}Cs e^2Qq/h and η values were evaluated from the observed widths $\Delta\nu_1$ and $\Delta\nu_2$ given by [15]

$$\begin{aligned} \Delta\nu_1 &= \frac{1}{14}\frac{e^2Qq}{h}(1-\eta), \\ \Delta\nu_2 &= \frac{1}{14}\frac{e^2Qq}{h}(1+\eta). \end{aligned} \tag{5}$$

Temperature dependences of the determined e^2Qq/h and η are shown in Figure 3.

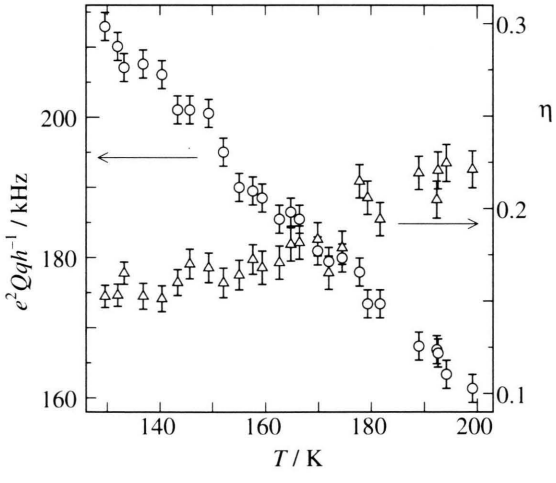

Fig. 3. Temperature dependences of e^2Qqh^{-1} (○) and η (△) of ^{133}Cs in Phase II of $Cs^{14}NO_2$.

^{15}N NMR Relaxation Time and Spectra in $Cs^{15}NO_2$

The relaxation mechanism for the ^{15}N T_1 minimum in $Cs^{15}NO_2$ observed in Phase II is attributable to the fluctuation of the chemical shift(CS) anisotropy at the ^{15}N nuclei. The observed T_1 value can be expressed as [14]

$$\frac{1}{T_1} \simeq \frac{3}{10}\Delta\omega^2 \frac{\tau}{1+\omega_N^2\tau^2}. \qquad (6)$$

where τ, ω_N, and $\Delta\omega$ denote the correlation time of the expected anionic motion, the ^{15}N Larmor angular frequency, and the line-width narrowed by the CS averaging, respectively. Equations (4) and (6) were fitted to the observed ^{15}N T_1 values, and the obtained best-fitted T_1 curve is shown in Figure 1. The evaluated activation parameters are given in Table 1.

Figure 4 shows the temperature dependence of ^{15}N NMR spectra observed in Phase I and II. All spectra of Phase II gave three principal CS components. This indicates that a motion giving no change of NO_2^- symmetry takes place in the above motional process.

A marked anomaly of the dielectric dispersion has been reported in the temperature and frequency ranges 58-130 K and 10^2-10^5 Hz, respectively, in Phase II [3, 4]. This indicates that the anionic motion in this phase is accompanied by a change of the electric-dipole direction of the NO_2^- ions. The activation energy E_a of 13.8 kJ mol^{-1} and the correlation time τ_0 of the order of 10^{-14} derived in the dielectric study at low-temperatures are close to the present NMR results in Table 1. These results suggest that the same motion is observed by these two different techniques.

By combining the results of the ^{15}N NMR lineshape and dielectric dispersion, we attribute this motion to a 180°-flip of the NO_2^- ion, in which its dipole flips about one of the two axes perpendicular to the molecular C_2-axis. This model can keep the ^{15}N three principal CS components unchanged through this motional process. The onset of this motion in Phase II is consistent with the orientational disorder of NO_2^- ions expected from thermal studies [3, 4]. Since the 180°-flip slows down at low temperatures, we can accept the proposed model of the freezing of NO_2^- orientation at the glass transition observed at *ca.* 40 K [3, 4].

It has been reported from the X-ray measurement that Phase II forms a rhombohedral lattice with the space group $R\bar{3}m$ and $Z = 1$ [1]. If this structure is applied, Cs nuclei are on the site of 1a or 1b, then spectra with $\eta = 0$ should be obtained. Moreover, in this structure ^{15}N NMR spectra with an axially symmetric CS tensor should be observed as reported in the rhombohedral phase of KNO_2 [9]. Since these expectations contradict with the present observations, we reinvestigated powder X-ray diffraction in this phase.

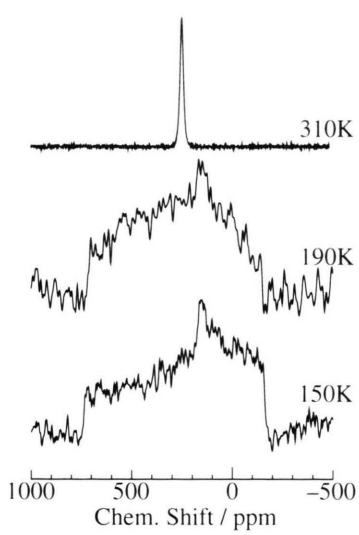

Fig. 4. ^{15}N NMR spectra observed at 30.56 MHz in Phase I and Phase II of $Cs^{15}NO_2$. The external reference of chemical shift is $^{15}NH_4^+$ (δ = −354 ppm) in a 4.5 M solution of $^{15}NH_4NO_3$ in 3 M hydrochloric acid.

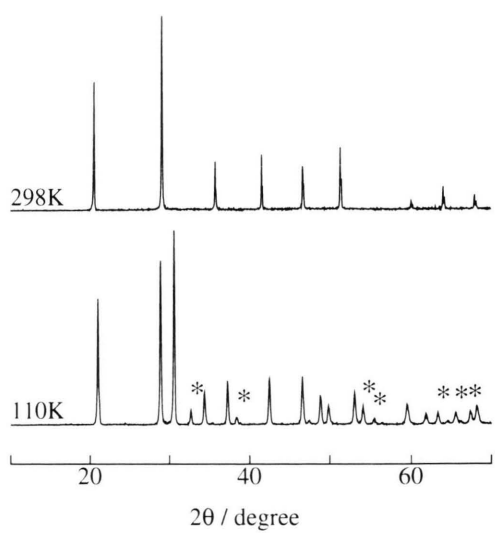

Fig. 5. X-ray powder diffraction patterns observed at 298 K in Phase I and at 110 K in Phase II of $CsNO_2$. Diffraction lines with asterisk are inexplainable by the reported rhombohedral lattice [1].

X-ray powder patterns observed at 298 K (Phase I) and 110 K (Phase II) are shown in Figure 5. The diffraction lines observed at 298 K were consistent with the reported data [1], whereas the pattern at 110 K gave seven extra peaks in a 2θ range of 10-70°, as shown in Fig. 5, which could not be indexed on the basis of the reported rhombohedral lattice [1]. Since these peaks were reproduced on repeated runs and undetectable in Phase I, they are characteristic of Phase II. The observed diffraction lines are explainable by a monoclinic system with $Z > 2$. This possibility does conform with the present results of ^{15}N and ^{133}Cs NMR spectra described above.

We measured the temperature dependence of the principal values of the ^{15}N CS tensor in $Cs^{15}NO_2$ and showed it in Figure 6. The calculation of the ^{15}N CS tensor in $Na^{15}NO_2$ [16, 17] afforded that the direction of the largest component δ_{33} is perpendicular to the molecular plane, the intermediate δ_{22} along the C_2-axis, and the smallest δ_{11} in the molecular plane. We can see that the absolute values of δ_{11} and δ_{33} gradually decrease upon heating in the high-temperature region, while δ_{22} changes little. This result suggests that there is an increase of the amplitude of NO_2^- libration about the C_2-axis upon heating or the onset of a new reorientation by a small angle about the axis. A similar motion has already been found in the low-temperature phase of $Rb^{15}NO_2$ [10] and $Tl^{15}NO_2$ [11].

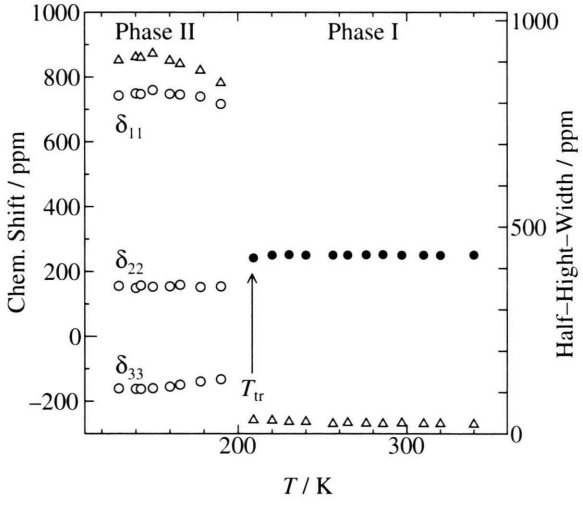

Fig. 6. Temperature dependences of three principal values (δ_{11}, δ_{22}, δ_{33}) (○) of the chemical shift tensor of ^{15}N observed in Phase II, isotropic-shift values in Phase I (●) and half-height-widths (△) of the observed spectra in $Cs^{15}NO_2$. T_{tr} denotes the phase transition temperature.

3.2. Phase I (Plastic Phase)

Phase I, which forms a CsCl-type cubic lattice [1, 12], contains isotropically disordered NO_2^- dipoles as predicted from structural and thermal studies [3, 4]. A T_1 maximum of ^{15}N and ^{133}Cs was observed around 250 and 350 K, respectively, as shown in Figure 1. We obtained a narrowed single ^{133}Cs and ^{15}N NMR spectrum at 340 K with a half-height width of *ca.* 300 Hz and *ca.* 730 Hz, respectively, as shown in Figs. 2 and 4, in the same order. The observed sharp ^{133}Cs spectrum with no satellite indicates spherically symmetric EFG at the Cs nuclei. The ^{15}N spectrum is quite analogous to those in $K^{15}NO_2$, $Rb^{15}NO_2$ and $Tl^{15}NO_2$ observed in the respective plastic phases. These results indicate the onset of isotropic reorientation of the NO_2^- ions in the plastic phases. The ^{15}N CS value of 252 ppm being independent of temperature is very close to 248, 249, and 239 ppm observed in potassium [9], rubidium [10], and thallium [11] salts, respectively.

^{133}Cs Relaxation Time in $CsNO_2$

The ^{133}Cs T_1 data observed in Phase I were inexplainable by contributions of two motional modes. We tentatively expressed the observed T_1 by the three relaxation times given by

$$\frac{1}{T_1} = \frac{1}{T_{1a}} + \frac{1}{T_{1b}} + \frac{1}{T_{1c}} \tag{7}$$

Here, T_{1a} contributes in the low-temperature range below 280 K, while T_{1c} at high temperatures above 450 K, and T_{1b} in the intermediate range. We assumed that these T_1 values can be written by (2) and (7) in which $\omega\tau \ll 1$ is assumed for T_{1a} and $\omega\tau \gg 1$ for T_{1c}. Applying (2),(4) and (7), we determined the best fitted T_1 curve shown in Fig. 1 and listed the obtained activation parameters in Table 1. We may assign T_{1a} to the NO_2^- reorientation about the C_2-axis which is expected to take place in Phase II as derived from the analysis of the CS anisotropy. This motion in Phase I seems to have a larger amplitude than in Phase II, and probably the 180°-flip of the NO_2^- ion is acceptable. The second component T_{1b} is attributable to the anionic isotropic reorientation which has been shown

from the ^{15}N spectrum analysis. The determined activation energy of 9±2 kJ mol^{-1} for this motion agrees well with 9.0 kJ mol^{-1} evaluated from ^{15}N T_1 in $Cs^{15}NO_2$, as discussed below. The third component T_{1c} can be assigned to the ionic self-diffusion. This assignment is supported by the analysis of ^{15}N T_2 and the temperature dependence of electrical conductivity given below.

^{15}N Relaxation Time in $Cs^{15}NO_2$

Temperature dependences of ^{15}N T_1 and T_2 observed in Phase I are shown in Figure 1. The observed ^{15}N T_2 values increased with temperature and became longer than 10 ms above 400 K. These T_2 values can be explained by the onset of ionic self-diffusion from the following calculation: We estimated the T_2 value from the magnetic dipolar linewidth ΔH of ^{15}N in a powder sample of Phase I, where isotropically rotating anions are assumed, using the relation [14]

$$\frac{1}{T_2} = \frac{\gamma_N}{2\pi}\sqrt{\langle \Delta H \rangle^2}, \tag{8}$$

$$\langle \Delta H \rangle^2 = \frac{3}{5}\hbar^2\gamma_N^2 I_N(I_N+1)\sum \frac{1}{r_{ij}^6} + \frac{4}{15}\hbar^2\gamma_{Cs}^2 I_{Cs}(I_{Cs}+1)\sum \frac{1}{r_{ik}^6}, \tag{9}$$

where γ_N, γ_{Cs}, I_N, and I_{Cs} denote the gyromagnetic ratios and spin quantum numbers of ^{15}N and ^{133}Cs nuclei, respectively. r_{ij} and r_{ik} are ^{15}N–^{15}N and ^{15}N–^{133}Cs inter-nuclear distances, respectively. The first and second terms in (9) are contributions from ^{15}N-^{15}N and ^{15}N-^{133}Cs magnetic dipolar interactions, respectively. Assuming the isotropically reorienting NO_2^- ions without self-diffusion, we evaluated a T_2 value of 5.5 ms from (8) and (9). The model of the NO_2^- isotropic reorientation and Cs^+ self-diffusion gives a calculated T_2 value of 33 ms. Since the T_2 > 10 ms observed above 400 K is much longer 5.5 ms for the model of isotropically rotating NO_2^- ions, this T_2 increase with temperature is attributed to the averaging of the interionic magnetic dipolar interactions due to the cationic self-diffusion. From the slope of the T_2 temperature dependence, we obtained an activation energy of 33±3 kJ mol^{-1} for the cationic self-diffusion.

A T_1 maximum was observed around 250 K at 30.42 MHz. We expressed the observed T_1 by

$$\frac{1}{T_1} = \frac{1}{T_{1a}} + \frac{1}{T_{1b}} \tag{10}$$

Here T_{1a} contributes in the low-temperature range below the T_1 maximum, while T_{1b} in the high-temperature range. We assumed that these T_1 values can be written by (4) and (10), in which $\omega\tau \ll 1$ is assumed for T_{1a} and $\omega\tau \gg 1$ for T_{1b}. Using (4), (6) and (10), we evaluated the best fitted T_1 curve as shown in Fig. 1 and determined the activation parameters given in Table 1. We assigned T_{1b} to the isotropic reorientation of NO_2^- ions as expected from the ^{15}N spectra analysis given above. It is noted that the activation energy of 9.0 kJ mol^{-1} for the isotropic reorientation is comparable to 10 and 12 kJ mol^{-1} reported for the same motion in KNO_2 [9], 6.2 kJ mol^{-1} in $RbNO_2$ [10], and 13.5 kJ mol^{-1}in $TlNO_2$ [11].

The motional mode contributing to T_{1a} is, accordingly, attributed to a new NO_2^- motion with an amplitude smaller than that of the isotropic reorientation. We may assign this model to the NO_2^- reorientation about its C_2-axis. The same motion gives the decrease in the ^{133}Cs T_1 in the same temperature range as discussed above.

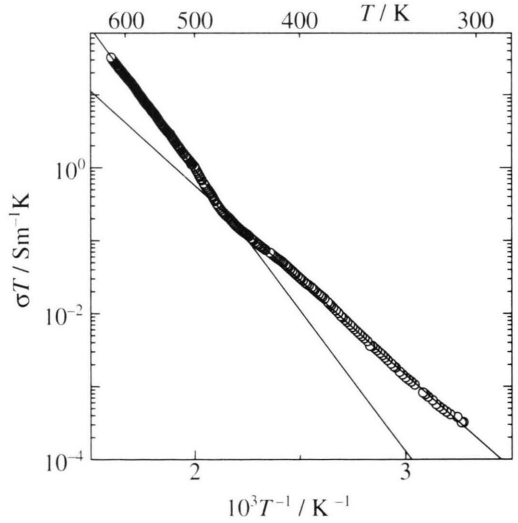

Fig. 7. Temperature dependence of the electrical conductivity σ observed at 1 kHz in Phase I of $CsNO_2$. The solid lines show the superimposed two conduction processes with activation energies of 50±5 and 74±5 kJ mol^{-1}.

Electrical Conductivity (σ)

We measured the electrical conductivity (σ) to confirm the presence of ionic self-diffusion. The temperature dependence of σT is shown in Figure 7. Upon heating, a rapid increase of σ to the order of 10^{-2} S m^{-1} was observed around 600 K. This clearly implies the presence of ionic conduction in conformity with the present NMR analysis.

Since the value of σT is proportional to the diffusion constant, if we apply the Nernst-Einstein relation, the diffusional activation energy can be derived from the slope of $\log \sigma T$ plotted against T^{-1}. We analyzed the data shown in Fig. 7, by assuming the presence of two conducting processes, which gave activation energies of 50±5 and 74±5 kJ mol^{-1}. The lower value agrees well with 47 kJ mol^{-1} obtained from the present NMR data analysis. The other value seems to stem from the barrier for anionic self-diffusion.

4. Conclusion

The anomalous increase of the heat capacity observed over a wide temperature range below the phase transition at 209.2 K in $CsNO_2$ was shown to be explained by the excitation of 180°-flip of NO_2^- ions in Phase II. This motion was determined from the temperature dependences of the ^{15}N NMR spectra, which retained the three kinds of different CS components in the whole temperature range of Phase II. The presence of this motion is supported by the reported data of the dielectric dispersion and relaxation [3, 4]. The ^{15}N and ^{133}Cs lineshapes indicating the absence of the C_3 site symmetry at the respective ions conflict with the reported structure $R\bar{3}m$ [1]. The X-ray diffraction patterns observed in this phase allowed us to attribute the structure of this phase to a monoclinic system, although the space group is unknown. This structure is consistent with the ^{15}N and ^{133}Cs NMR spectra observed in the present study.

In the plastic phase (Phase I) having a CsCl-type cubic lattice, the anionic isotropic reorientation and a new motion attributable to the NO_2^- reorientation about its C_2-axis, were derived from ^{15}N and ^{133}Cs NMR T_1. The activation energy of 9.0 kJ mol^{-1} determined for the isotropic reorientation are close to 13.5 kJ mol^{-1} obtained in $TlNO_2$ [11] having a CsCl-type cubic structure, and 10 and 12 kJ mol^{-1} in KNO_2 [9], and 6.2 and 8.5 kJ mol^{-1} in $RbNO_2$ [10], both forming the NaCl-type cubic lattice. On the other hand, the obtained activation energy of 47 kJ mol^{-1} for cationic self-diffusion derived from T_1 became the same as that in $TlNO_2$ [18, 19], whereas it is much smaller than 110 kJ mol^{-1} in $RbNO_2$ [10]. This difference in the diffusional barriers can be attributed to the difference in the diffusional process in which ions can directly jump to the nearest vacant site in the CsCl-type lattice, whereas two successive jumps over a high barrier are needed in the NaCl-type lattice [20 - 22].

Acknowledgement

We are grateful to Dr. Y. Onoda and Dr. M. Tansho in National Institute for Research in Inorganic Materials for the use of the MSL-400 spectrometer. This work was partly supported by a Grant-in-aid for Scientific Research No. 06453055 from the Ministry of Education, Science and Culture, Japan.

[1] P. W. Richter and C. W. F. T. Pistorius, J. Solid State Chem. **5,** 276 (1972).
[2] S. C. Mraw, R. J. Boak, and L. A. K. Staveley, J. Chem. Thermodyn. **8,** 1001 (1976).
[3] K. Moriya, T. Matsuo, and H. Suga, Chem. Phys. Lett. **82,** 581 (1981).
[4] K. Moriya, T. Matsuo, and H. Suga, J. Phys. Chem. Solids, **44,** 1103 (1983).
[5] K. Moriya, T. Matsuo, and H. Suga, Thermochim. Acta, **132,** 133 (1988).
[6] S. C. Mraw, R. J. Boak, and L. A. K. Staveley, J. Chem. Thermodyn. **10,** 359 (1978).
[7] K. Moriya, T. Matsuo, and H. Suga, Bull. Chem. Soc. Japan **61,** 1911 (1988).
[8] K. Moriya, T. Matsuo, H. Suga, and S. Seki, Chem. Lett. 1427 (1977).
[9] M. Kenmotsu, H. Honda, H. Ohki, R. Ikeda, T. Erata, A. Tasaki, and Y. Furukawa, Z. Naturforsch.**49a,** 247 (1994).
[10] H. Honda, M. Kenmotsu, H. Ohki, R. Ikeda, and Y. Furukawa, Ber. Bunsenges. Phys. Chem.**99,** 1009 (1995).
[11] H. Honda, S. Ishimaru, N. O-Yamamuro, and R. Ikeda, Z. Naturforsch. **50a,** 871 (1995).

[12] J. N. Sherwood, The Plastically Crystalline State, John Wiley & Sons, Chichester 1979.
[13] D. Hohlwein, A. Hoser, and W. Prandl, Z. Kristallogr. **177,** 93 (1986).
[14] A. Abragam, The Principles of Nuclear Magnetism, Oxford University Press, London 1961.
[15] M. H. Cohen and R. Reif, Solid State Phys. **5,** 321 (1957).
[16] R. E. Wasylishen, R. D. Curitis, K. Eichele, M. D. Lumsden, G. H. Penner, W. P. Power, and G. Wu, NATO ASI Ser. Ser. C, **386,** 297 (1993).
[17] J. Mason, NATO ASI Ser. Ser. C **386,** 449 (1993).
[18] Y. Furukawa and H. Kiriyama, Chem. Phys. Lett. **93,** 617 (1982).
[19] Y. Furukawa, H. Nagase, R. Ikeda, and D. Nakamura, Bull. Chem. Soc. Japan. **64,** 3105 (1991).
[20] M. Tansho, Y. Furukawa, D. Nakamura, and R. Ikeda, Ber. Bunsenges. Phys. Chem. 96, 550 (1992).
[21] N. E. Byer and H. S. Sack, Phys. Rev. Lett. 17, 72 (1966).
[22] R. J. Quigley and T. P. Das, Solid State Commun. 5, 487 (1967).